10.4

DETERMINATION OF METHANE EMISSIONS FROM LIVESTOCK AT THE FARM SCALE USING OBSERVED METEOROLOGICAL AND CONCENTRATION PROFILES AND INVERSE MODELLING TECHNIQUES

Neil Gimson[(1)#], Gordon Brailsford[(1)], Tony Bromley[(1)], Keith Lassey[(1)], Ross Martin[(1)], Rowena Moss[(1)], Marek Uliasz[(2)]

[(1)] National Institute of Water & Atmospheric Research, Wellington, New Zealand
[(2)] Department of Atmospheric Science, Colorado State University, Fort Collins, Colorado

1 INTRODUCTION

Agricultural greenhouse gas emissions account for 50% of New Zealand's CO_2-equivalent emissions, a prominence unmatched by the emissions profile of any other Annex I party to the United Nations Framework Convention on Climate Change. Methane emitted by livestock through enteric fermentation accounts for one third of NZ's CO_2-equivalent emissions. The methane inventory in NZ is based on per-animal emission rates, scaled up to provide regional and national totals. Top-down emissions estimation techniques are investigated here and compared with inventory totals, with the aim of enhancing confidence in emission flux estimates.

In principle, methane concentrations increase as air blows across a region grazed by livestock. If vertical profiles of methane are measured both upwind and downwind, the contrast between them reflects the strength of the intervening sources. At the farm scale – distances of tens to hundreds of metres, areas of several hectares – near-surface contrasts in methane are easily detectable. This enables individual farm emissions to be assessed, and potentially provides a tool to verify emission mitigation measures provided that sufficient precision is attainable.

2 FARM-SCALE EXPERIMENTS

Several measurement campaigns have been undertaken over the last two years, with some variations in experimental design. In this paper, the focus is on a field campaign which took place in the Wairarapa region of New Zealand on 18 June 2003.

2.1 *Meteorological Measurements*

The Wairarapa region consists of an inland plain with rolling country to the south. In the southeast are the steep but low Aorangi Mountains, rising to 980m. The region is bounded by the Rimutaka and Tararua ranges to the west, to 940 m and 1600 m respectively. The weather of the Wairarapa is controlled to a large extent by these ranges. When westerly winds blow across the region the ranges shelter the lowland areas, giving high temperatures and dry weather. In southerly and easterly situations rainfall is enhanced as the air masses are forced to ascend over the ranges.

The field campaign of 18 June 2003 took place on a dairy farm on the flat plain south of Greytown in South Wairarapa. The Tararua range is approximately 10 km to the west, and the Aorangi Mountains some 40 km to the east and southeast. The experimental paddock was open to wind flow from all directions, with only one or two large trees just west of the main observation and sampling position. The flow over the paddock during the experiment period was from the northeast over clear flat grassland. The nearest obstacles (a line of trees) were about 1 km to the north.

Three ground-based automated weather stations were deployed in the area. These provided wind speed and direction, temperature, solar radiation and relative humidity data as ten-minute averages for the days leading up to and throughout the experiment. In addition to the ground-based measurements a tethersonde was attached to a Helikite to supply continuous meteorological data at the highest air-sampling level above the study area (at 50 m above ground level; see Figure 1).

2.2 *Air Sampling*

A rectangular paddock of 1.76 hectares was stocked with 160 dairy cows on the morning of the experiment. This stocking density was part of the normal farm practice, and not artificially increased for the benefit of the field experiment. Air samples were collected using bag samplers, averaged over five 40-minute periods. Five sampling locations were along a line transverse to the wind direction 70 m downwind of the paddock, providing a transect that traversed the entire plume, at 1.5 m elevation. At a midpoint across the paddock on this transect a 6 m

Corresponding author address: Neil R. Gimson, NIWA Ltd., Private Bag 14-901, Kilbirnie, Wellington, New Zealand. E-mail: n.gimson@niwa.co.nz.

mast was used to collect air samples at heights of 1.5, 3 and 6 m. The Helikite, tethered at this location, raised tubing for sampling air at (nominal) heights of 12, 25 and 50 m above ground level. The average winds observed during the five sampling periods are shown in Table 1. Wind speeds were quite low during the field trial, from the NE and NNE, with direction uniform with height.

Figure 1: Helikite being raised with suspended radiosonde and sampling tubes at several heights.

Period	Start time (NZST)	Surf. WS (m/s)	Surf. WD (deg)	Kite WS (m/s)	Kite WD (deg)
A	1330	1.6	29	2.2	20
B	1410	2.3	45	3.1	35
C	1450	2.5	46	3.6	39
D	1530	2.4	46	3.4	45
E	1610	1.5	46	3.6	41

Table 1: Average meteorological conditions during the five 40-minute periods on 18 June 2003.

2.3 *Gas Analysis*

The mixing ratio of methane was determined by gas chromatography (HP5890 Series II) using a flame ionization detector with packed column of 5A molecular sieve (Lowe et al., 1994). Results are reported against the National Institute of Standards and Technology (NIST) reference scale. Ten repeat measurements were made of each sample, with each one bracketed by a reference gas measurement. Concentration measurements were normalized to dry air, removing water vapour using a back-flushed nafion dryer and magnesium perchlorate.

3 METHANE DISPERSION MODELLING

Dispersion modelling techniques are employed to ascertain the origins of the sampled air and to estimate the paddock emission fluxes which gave rise to the observed methane concentrations. A Lagrangian particle dispersion (LPD) model, run in an inverse mode, permits quantification of the source-receptor relationship. The advantages of running in inverse mode are (i) computational efficiency, where model particles are released from observation points backward in time rather than from source areas forward in time; and (ii) the emission patterns may be specified as a post-processing step, once the origins of the air have been determined.

3.1 *Surface-Layer Wind Profiles*

The meteorological conditions were assumed to be horizontally uniform, but varying vertically and with time. Standard meteorological parameters were available at the nearest ground-based weather stations and, during the air sampling periods, at the Helikite level. Surface-layer similarity theory is used to interpolate between these two levels, to extrapolate above them as necessary, and to derive a complete profile of wind, temperature and turbulent velocity fluctuation parameters.

Under unstable conditions, given the wind speed (U_1 and U_2) at the two measurement levels (z_1 and z_2), surface-level temperature (T) and net surface heat flux (H), the following formulae are iterated to derive the friction velocity (u^*), Obukhov length (L) and roughness length (z_0).

$$U_2 - U_1 = \frac{u^*}{k}\left\{\ln\left(\frac{z_2}{z_1}\right) - \psi_2 + \psi_1\right\}, \quad (1)$$

$$U_1 = \frac{u^*}{k}\left\{\ln\left(\frac{z_1}{z_0}\right) - \psi_1\right\}, \quad (2)$$

$$\psi_j = 2\ln\left(\frac{1+x_j}{2}\right) + \ln\left(\frac{1+x_j^2}{2}\right) - 2\tan^{-1}(x_j) + \frac{\pi}{2}, \quad (3)$$

$$x_j = \left(1 - \frac{15 z_j}{L}\right)^{1/4} \qquad j = 1, 2, \quad (4)$$

$$L = \frac{-c_p \rho T u_*^3}{kgH}. \quad (5)$$

Wind direction is assumed constant with height. The wind speed at any height may then be calculated using equation (1) or (2), once the surface-layer parameters have been determined. For dispersion modelling, the mixing height (h) and convective velocity scale (w^*) are calculated, being related by

$$w^* = \left(\frac{gHh}{T} \right)^{1/3} . \qquad (6)$$

The velocity-profile formula was originally developed by Businger *et al.* (1971), and the universal stability function (ψ) formula by Paulson (1970). Equations (5) and (6) are textbook definitions.

3.2 *Particle Dispersion Modelling and Influence Functions*

The LPD model was developed by Uliasz (1993) for mesoscale applications, and has been used to model dispersion of methane and determine its emission fluxes on the regional scale in New Zealand (Gimson and Uliasz, 2003). In the slightly modified form used here, the standard deviations of the wind velocity components are required as inputs. These are given by Panofsky *et al.* (1977) as

$$\frac{\sigma_u}{u^*} = \frac{\sigma_v}{u^*} = \left(12 + 0.5 \frac{h}{|L|} \right)^{1/3} \qquad (z \le h), \qquad (7)$$

$$\frac{\sigma_w}{w^*} = 0.96 \left(3\frac{z}{h} - \frac{L}{h} \right)^{1/3} \qquad (z \le 0.03h), \qquad (8a)$$

$$\frac{\sigma_w}{w^*} = \min \left\{ 0.96 \left(3\frac{z}{h} - \frac{L}{h} \right)^{1/3} , 0.763 \left(\frac{z}{h} \right)^{0.175} \right\}$$

$$(0.03h \le z \le 0.4h), \qquad (8b)$$

$$\frac{\sigma_w}{w^*} = 0.722 \left(1 - \frac{z}{h} \right)^{0.207} \qquad (0.4h \le z \le 0.96h), \qquad (8c)$$

$$\frac{\sigma_w}{w^*} = 0.37 \qquad (0.96h \le z \le h). \qquad (8d)$$

These components are allowed to fall linearly to zero between heights h and $1.1h$. To characterize the origins of the sampled air, model particles are released from receptors (air sampling points) and dispersed backward in time through the turbulent flow. The influence function is merely a gridded representation of the density of particles reaching the surface.

The source-receptor relationship may be expressed as (Uliasz, 1993)

$$C_D = \int_{t_1}^{t_2} \int_{Paddock} QC^* dxdydt \Big|_{z=0} + C_0 , \qquad (9)$$

where C_D is the methane concentration downwind of the paddock. C_D depends on the upwind concentration (C_0, assumed here to be uniform) and emission flux (Q) from the surface of the intervening region. The time interval (t_1, t_2) delimits the contributing emissions – the concentrations are averaged over some later period. The fluxes in equation 9 are thus 'weighted' by the influence function (C^*), which depends on the location and timing of the profile sampling. The influence function, which essentially depicts a probability distribution for air originating at the surface, may not reach, or may extend beyond the paddock.

Figure 2 shows examples of time-averaged influence functions for periods A and E. Although the mean wind speed is similar in each case, period E occurs closer to sunset on a winter day, leading to less unstable atmospheric conditions and longer, more coherent 'plumes'.

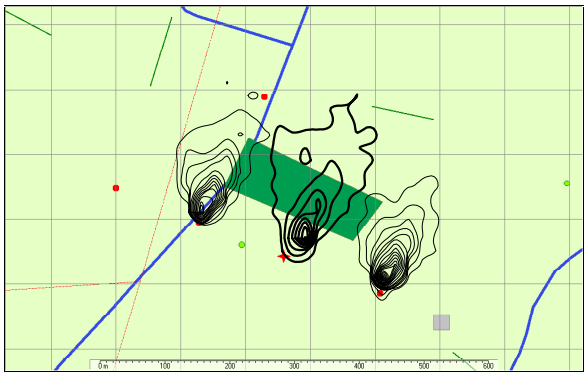

(a)

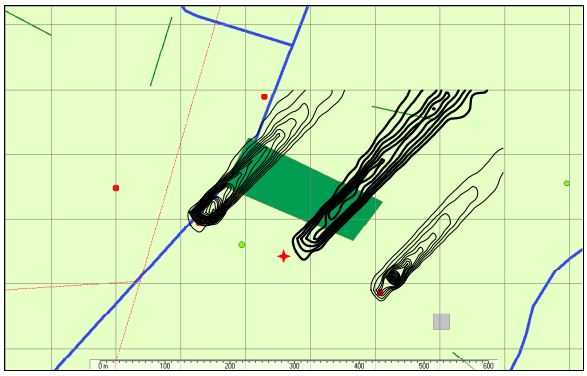

(b)

Figure 2 Surface influence functions for the 25 m Helikite sample (bold contours) and for two of the bag samplers (locations denoted by small circles). The Helikite sampling and meteorological monitoring sites are denoted by a cross. The dairy paddock is shaded. The influence functions have arbitrary units and are time-averaged over (a) Period A and (b) Period E.

3.3 *Estimates of Emission Rates*

A simple linear regression of the downwind methane measurements on the influence function (averaged over the paddock) provides an estimate of the paddock methane flux and the 'background' methane concentration. These are the slope and intercept, respectively, of the regression. The upwind methane concentrations are not input into the calculation but are used for comparison with the results.

Using all observations as data points in the linear regression results in an unrealistically wide variation of calculated emission rates between observation periods, with high background concentrations calculated, and low correlations between observed and modelled concentrations. However, a wide variation in methane concentration at the bag samplers is observed, with large values occurring when the sampled air appears not to have originated from the paddock of interest. The methane may have arisen from alternative sources (livestock in other paddocks, or the surrounding soil), or the variation close to the surface is not well explained by the model. Subsequent field campaigns have used bag samplers at levels higher than 1.5 m to remove the effects of very small and variable surface footprints.

If the observations from the bag samplers are disregarded, the calculated emission rates are as shown in Table 2. In this case, the calculated background methane concentrations (determined largely by the Helikite observations at 25 and 50 m) are closer to those observed upwind. Also, the per-animal estimated emission rates – at least, for Periods B, D and E – are closer to those calculated using inventory methodologies. However, the neglect of some observations is slightly arbitrary and a closer investigation into the reasons for the high methane concentrations observed at the bag samplers is required. (Note that the correlation coefficients, though improved, are not meaningful when there are few data points).

Time Period	Emission Rate (gCH_4/day)	Calculated Background CH_4 (ppbv)	*R*	Observed Background CH_4 (ppbv)
A	660	1784	0.6	1781
B	311	1784	0.9	1793
C	4621	1778	1.0	1798
D	324	1813	0.8	unknown
E	342	1839	0.8	1892

Table 2: Emission rates from inverse modelling for 18 June 2003. Methane fluxes are given as a per-animal emission rate. The observed background methane is taken from the 6 m mast. R denotes the correlation coefficient.

Given the influence function, emission fluxes and background methane calculated in the model, profiles of methane may be derived and compared with those observed. An example is shown for Period E in Figure 3. Close to the paddock, the emitted methane is contained in a layer a few metres deep.

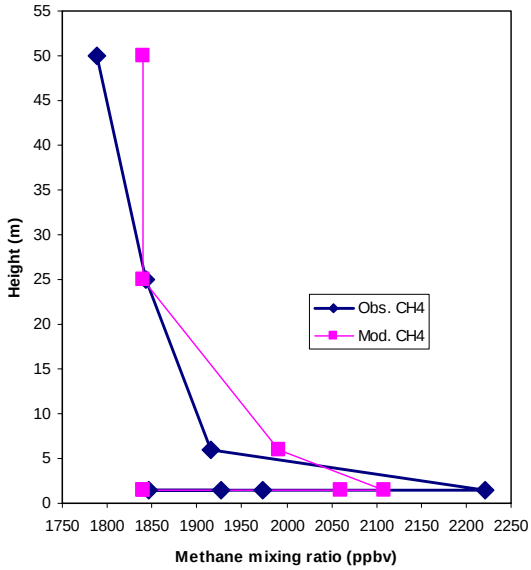

Figure 3: Comparison of observed and modelled methane during Period E, on 18 June 2003, for a calculated emission rate of 342 g/animal/day. Note several of the data points are 1.5 m above ground level, and no concentration at 12 m was obtained for this period.

4 DISCUSSION

The dairy cows in the autumn experiment of Lassey *et al.* (1997) emitted methane in the range 229-313 gCH_4/day per animal. The 'best' results obtained from the inverse modelling here are around 50% higher than the middle of this range, but this should be interpreted as good model performance. A more rigorous inventory-based estimate would utilize cows' liveweight, productivity, feed intake and feed quality, and also account for possible co-located methane sources such as cow excrement.

An important aspect of this work is the validation of the dispersion model and associated analysis techniques. This will include field campaigns where, in place of livestock, an artificial source of methane will be installed. Methane will be released at a uniform, metered rate from a tank through a lattice of tubes in the paddock to simulate a distribution of cows. An identical measurement campaign and modelling exercise will be carried out to validate the inferred methane flux against the known source strength. In addition, work is in progress to validate the model against the field data of Flesch *et al.* (2004).

Given the precision attainable in the observations of meteorological parameters and trace-gas concentrations, the largest uncertainties are undoubtedly in the model. This includes the formulation and performance of the LPD model, and also the applicability of the conceptual model of uniform meteorology with a 'standard' surface-layer structure and the assumption of emissions from the paddock of interest and nowhere else. It is hoped that these uncertainties will be reduced through refinements to the modelling approach based on the validation studies currently underway. By adopting a Bayesian statistical approach, combining inventory-based calculations with the top-down methods described here, the resulting emission flux uncertainties should, in the end, be less than those arising from either technique individually.

Thus far, dispersion modelling of current field experiments has been used to guide future campaigns. The influence function provides a useful insight into the origins of sampled air, particularly its distance and direction from the sampling point, and provides guidance on the usefulness of near-surface and upwind sampling.

Examination of results from several field campaigns demonstrates that the meteorological conditions are critical to the success of the experiment. To discern an upwind-downwind contrast in methane concentrations, there must be a well-defined wind direction, as opposed to calm winds of variable direction. But consideration of dispersion patterns indicates that requirements should be somewhat stricter, and that more definitive results are obtained when the surface wind speed reaches, say, 4-5 m/s.

5 CONCLUSIONS

A full analysis of experimental and modelling results, following any necessary refinements to both aspects, will provide confidence limits based upon measurement and modelling uncertainties. At that point, an assessment of the efficacy of the present measurement/modelling approach as a verifier of emission inventory estimates (or as an improver of confidence intervals in the Bayesian approach) will be able to be made. A much stricter requirement of the approach will be an ability to validate emissions mitigation claims.

ACKNOWLEDGMENTS

This research was carried out with funding from the NZ Foundation for Research, Science and Technology, under contract C01X0204.

REFERENCES

Businger, J. A., Wyngaard, J. C., Izumi, Y. and Bradley, E. F., 1971: Flux-profile relationships in the atmospheric surface layer. *J. Atmos. Sci.*, **18**, 181-189.

Flesch, T. K., Wilson, J. D., Harper, L. A., Crenna, B. P. and Sharpe, R. R., 2004: Deducing ground-to-air emissions from observed trace gas concentrations: a field trial. *J. Appl. Meteor.*, **43**, 487-502.

Gimson, N. R. and Uliasz, M., 2003: The determination of agricultural methane emissions in New Zealand using receptor-oriented modelling techniques. *Atmos. Environ.*, **37**, 3903-3912.

Lassey, K. R., Ulyatt, M. J., Martin, R. J., Walker, C. F. and Shelton, I. D., 1997: Methane emissions measured directly from grazing livestock in New Zealand. *Atmos. Environ.*, **31**, 2095-2914.

Lowe, D. C., Brenninkmeijer, C. A. M., Brailsford, G. W., Lassey, K. R. and Gomez, A. J., 1994: Concentration and 13C records of atmospheric methane in New Zealand and Antarctica: evidence for changes in methane sources. *J. Geophys. Res.*, **99**, 16913-16925.

Panofsky, P. A., Tennekes, H., Lenschow, D. H. and Wyngaard, J. C., 1977: The characteristics of turbulent velocity components in the surface layer under convective conditions. *Bound.-Layer Meteor.*, **11**, 355-361.

Paulson, C. A., 1970: The mathematical representation of wind speed and temperature profiles in the unstable atmospheric surface layer. *J. Appl. Meteor.*, **9**, 857-861.

Uliasz, M., 1993: The atmospheric mesoscale dispersion modeling system. *J. Appl. Meteor.*, **32**, 139-149.